Impact of GSG probe to pads contact repeatability for on-wafer RF measurements

Cerine Mokhtari, Mohamed Sebbache, Vanessa Avramovic, Christophe Boyaval, Gilles Dambrine, Kamel Haddadi

HAL Id: hal-03404613
https://hal.science/hal-03404613

Impact of GSG Probe to Pads Contact Repeatability for On-Wafer RF Measurements

Cerine Mokhtari
Centre National de la Recherche Scientifique (CNRS), Université Lille, USR 3380 - IRCICA
Univ. Lille, CNRS, Centrale Lille, Univ. Polytechnique Hauts-de-France, UMR 8520 - IEMN - Institut d'Electronique de Microélectronique et de Nanotechnologie
Lille, France
cerine.mokhtari@iemn.fr

Mohamed Sebbache
Centre National de la Recherche Scientifique (CNRS), Université Lille, USR 3380 - IRCICA
Univ. Lille, CNRS, Centrale Lille, Univ. Polytechnique Hauts-de-France, UMR 8520 - IEMN - Institut d'Electronique de Microélectronique et de Nanotechnologie
Lille, France
mohamed.sebbache@iemn.fr

Vanessa Avramovic
Centre National de la Recherche Scientifique (CNRS), Université Lille, USR 3380 - IRCICA
Univ. Lille, CNRS, Centrale Lille, Univ. Polytechnique Hauts-de-France, UMR 8520 - IEMN - Institut d'Electronique de Microélectronique et de Nanotechnologie
Lille, France
vanessa.avramovic@iemn.fr

Christophe Boyaval
Centre National de la Recherche Scientifique (CNRS), Université Lille, USR 3380 - IRCICA
Univ. Lille, CNRS, Centrale Lille, Univ. Polytechnique Hauts-de-France, UMR 8520 - IEMN - Institut d'Electronique de Microélectronique et de Nanotechnologie
Lille, France
christophe.boyaval@iemn.fr

Gilles Dambrine
Centre National de la Recherche Scientifique (CNRS), Université Lille, USR 3380 - IRCICA
Univ. Lille, CNRS, Centrale Lille, Univ. Polytechnique Hauts-de-France, UMR 8520 - IEMN - Institut d'Electronique de Microélectronique et de Nanotechnologie
Lille, France
gilles.dambrine@univ-lille.fr

Kamel Haddadi
Centre National de la Recherche Scientifique (CNRS), Université Lille, USR 3380 - IRCICA
Univ. Lille, CNRS, Centrale Lille, Univ. Polytechnique Hauts-de-France, UMR 8520 - IEMN - Institut d'Electronique de Microélectronique et de Nanotechnologie
Lille, France
kamel.haddadi@iemn.fr

Abstract— **Improving the contact repeatability for on-wafer measurements is required to address accurate characterization of microwave and millimeter-wave extreme impedance devices foreseen in future RF semi-conductor industry. In this effort, residual error terms introduced by conventional on-wafer probe measurements are quantified in the frequency range 50 MHz – 67 GHz. In particular, two sets of measurements considering movements of the probes in the Z-direction only and in X-Y-Z directions are considered. Controlling the probe in the XY axis showed better results in terms of repeatability, more than 10 times à 10 GHz and more than 5 times à 60 GHz. The residual error terms are propagated to determine the measurement uncertainty on the complex impedance of capacitances theoretically tested. Capacitance value of 1 fF measured at 10 GHz was measured with an error around 80 %. Moving the probe on the Z-direction only demonstrated that, if the X and Y movements of the probe are theoretically controlled, the error could be reduced to ~7%. In addition, preliminary design and fabrication of a new compact on-wafer probe station built up with nanorobotics is proposed. Both chuck and RF probes are equipped with nano-positioning stages operating in close loop operation.**

Keywords— ***On-wafer measurements, ground-signal-ground (GSG) probes, line-reflect-reflect-match (LRRM) calibration, two-port calibration, vector network analyzer (VNA).***

I. INTRODUCTION

More and more accurate radio frequency (RF) on-wafer probing techniques are required to address future semi-conductor industry needs [1]. In particular, there is an urgent need to assess the traceability and the variability of agile micro- and nano-devices foreseen in future 5G applications and beyond [2]-[3]. A typical RF device characterization set-up consists of a vector network analyzer (VNA), a probe station with a pair of microwave ground-signal-ground (GSG) probes aligned manually or automatically through a microscope or a camera system onto calibration substrate and test devices [4]. Errors such as drift, stability, and contact repeatability degrade the measurement accuracy, especially as the frequency is raised [5]-[8]. In particular, measurements are sensitive to X, Y, Z, and Θ positioning of the GSG probe contacts with respect to calibration standards and devices pads [9].

The main objective of this work is twofold. First, we develop a framework to propagate the measurement uncertainty inherent to the on-wafer probing set-up on the impedance to be quantified. These results are instructive as they suggest that conventional measurement systems using manual positioning stages induce large measurement uncertainties for accurately characterize extreme impedances. Then, in a second step, we introduce the preliminary design and fabrication of a new generation of on-wafer probe station to tackle the issue inherent to the contact repeatability. In this configuration, both GSG probes and chuck are equipped with close-loop piezo-based nano-positioning stages with nanometer (nm) positioning accuracy to surpass by three orders of magnitude the performance commonly found with mechanical positioning stages. In addition, the on-wafer probe station is interfaced with a streamline Keysight Technologies® vector network analyzer (VNA) operating up to 53 GHz to achieve a compact solution and therefore reduce non-systematic errors.

II. METHODOLOGY FOR THE DETERMINATION OF RESIDUAL CALIBRATION ERROR TERMS

A. On-wafer probing set-up and configuration

The experimental setup involves a MPS150 conventional on-wafer probe station from Cascade Microtech® equipped with a pair of 100 μm pitch GSG Infinity® probes. The VNA used for the S-parameters measurements is an E8361A (PNA) operating up to 67 GHz from Keysight Technologies®. The intermediate frequency bandwidth (IFBW) is set to 100 Hz and the RF signal source to -10 dBm. The frequency range is set from 50 MHz to 67 GHz with a frequency step of 50 MHz

(1340 points). Two 1.85 mm coaxial RF cables from Gore® are used to connect the probes to the VNA. The calibrations are done on the impedance standard substrate (ISS) PN 101-190 from Form-Factor®. The software Wincal® is used to ensure the LRRM calibration algorithm. The software also provides the full 12 calibration error terms namely directivity E_D, transmission tracking E_T, reflection tracking E_R, source match E_S, load match E_L, cross-talk E_T and E_X isolation (neglected) as represented in Fig. 1 for the forward path.
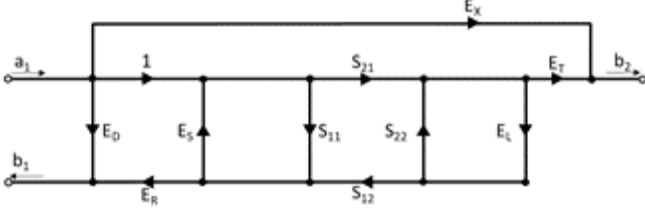

Fig. 1. Forward 12-term on-wafer probe error model.

In Fig. 1, the calibration term errors relate the S-parameters S_{ij} of the device under test (DUT) to the S-parameters S_{ijM} measured by the VNA ($S_{11M} = \frac{b_1}{a_1}$, $S_{21M} = \frac{b_2}{a_1}$) for the forward direction.

B. Vector calibration

Two sets of measurements are carried out on the same day in a controlled environment with temperature variations less than ± 1°, stable ambient hygrometry set to 50 % and anti-vibration building. On the first half of the day, we did a first set of measurements called Z-analysis; on the second half of the day we did the second set of measurements called XYZ-analysis.

The Z-analysis is performed according to the following protocol:

- 10 LRRM calibrations are performed independently.

- For each standard, e.g., short, we fixed the alignment of the probes on the X, Y and Z axis. Once the contact is correctly done, we move the probes on the Z axis only using the manual handle of the probing station in order to perform 10 successive measurements of the short standard. We repeat the same procedure for the other standards.

- 10 LRRM calibration files are created.

The XYZ-analysis is performed as follow:

- 10 LRRM calibrations are performed independently by moving the probes according to the standards on all the axis (displacement in the centimeter range).
- 10 LRRM calibration files are created.

This procedure allows us to study the influence of the manual alignment of the probes in the X, Y and Z directions.

From each of the ten calibration files, we compute the 12 calibration error terms usin Wincal®.

C. Determination of the residual calibration error terms

The residual calibration error terms, that correspond mathematically to the complex standard deviations of the error calibration terms, are the signatures of (i) mainly the mechanical repeatability of the probe to contact pads, (ii) non-systematic errors occurring between the measurements (instrument drift, environment variations). The residual data are computed for each error term as follows

$$Residual = \sqrt{\frac{1}{N-1}\sum_{i=1}^{N}\{(x_i - \bar{x})^2 + (y_i - \bar{y})^2\}} \qquad (1)$$

where x_i and y_i are the real and imaginary component of the i-th error term value, $\bar{x}$ and $\bar{y}$ the means values of real and imaginary parts of the error terms respectively, and $N = 10$ the number of measurements. The residual calibration error terms indicate how spread are the values from the mean data. Consequently, the standard deviation must be kept low to ensure the repeatability of the measurements.

In addition, to make the link between residual calibration error terms and the measured S-parameters of the calibration standards, we compute also the standard deviations of the measured S-parameters of the four calibration standards used for LRRM calibration, namely short, open, load and thru. All data analysis is done through MATLAB® software.

It has to be mentioned that the method presented is different from the well-known approach developed by D. Rytting [10] in which all sources of uncertainties are considered independently. In particular, systematic and non-systematic (noise, connector repeatability, cable stability, noise drift and stability) errors require a set of specific measurements to identify and quantify each error contribution. In our case, we consider a global approach with the main objective to quantify the impact of manual positioning (Z and XYZ) directly on the complex impedance to be measured. In the following, a method is proposed to propagate the measurement uncertainty brought by the residual calibration terms on the impedance in a one-port measurement scenario. Indeed, although the method can be generalized to any two-port network, we focus on the following on the measurement of complex impedance / complex reflection coefficient only.

III. EXPERIMENTAL SET-UP AND VALIDATION

The method developed in section II is applied to derive the measurement uncertainties considering an ISS in the frequency range 50 MHz – 67 GHz.

A. Standard deviation computed on microwave signals

Fig. 2 shows the standard deviations computed from the measured complex reflection coefficients (raw data) on the standards, considering 10 calibrations for XYZ-analysis and Z-analysis.
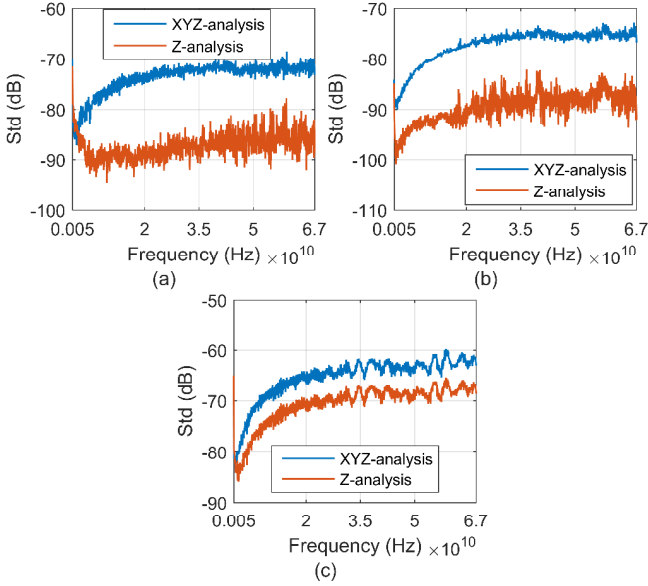
Fig. 2. Standard deviations obtained from measured complex reflection coefficients on the impedance standard substrate (ISS). (a) open. (b) load. (c) short.

From Fig. 2, we demonstrate that XYZ-analysis results in degradation of the measurement repeatability in contrast with the Z-analysis. We observe that for both methods, the repeatability quality decreases when the frequency rises, up to 20 GHz. From 20 to 50 GHz, the repeatability of the measurements does not change significantly due to other source of uncertainties (e.g., instrumental drift) that become predominant. Consequently, measurement uncertainties in the lower regime (< 20 GHz) can be improved by suitable accurate probing techniques. In the upper frequency regime, complementary strategies to identify and remove sources of uncertainties must be considered.

The individual errors presented in Fig. 2 and brought by the limited probe to pad repeatability are combined altogether to impact the overall vector calibration discussed in the next sub-section.

B. Residual calibration error terms

The residual calibration error terms have been computed for both XYZ-analysis and Z-analysis in the range 50 MHz – 67 GHz. Tables I and II present the data obtained for the test frequencies 1, 10, 30 and 60 GHz. The Z-analysis shows better results in terms of repeatability. For example, at 10 GHz, the residual directivity error term is increased by a factor around 12 between Z and XYZ-analysis.

TABLE I - 3σ STANDARD DEVIATIONS COMPUTED AT 1GHZ, 10GHZ, 30GHZ AND 60GHZ - Z-ANALYSIS

Residual error	1GHz	10GHz	30GHz	60GHz
	3 σ	*3 σ*	*3 σ*	*3 σ*
Directivity δ_1	3.7707e-05	5.9740e-05	1.3925e-04	1.4346e-04
Reflection tracking τ_1	2.0059e-04	1.6715e-04	2.8929e-04	3.0141e-04
Transmission tracking τ_2	1.1613e-04	1.3879e-04	2.8849e-04	3.1446e-04
Source match μ_1	1.3467e-04	2.4666e-04	9.7239e-04	1.7725e-03
Source match μ_2	1.0131e-04	2.7117e-04	9.7285e-04	1.7873e-03

TABLE II - 3σ STANDARD DEVIATIONS COMPUTED AT 1GHZ, 10GHZ, 30GHZ AND 60GHZ - XYZ-ANALYSIS

Residual error	1GHz	10GHz	30GHz	60GHz
	3 σ	*3 σ*	*3 σ*	*3 σ*
δ_1	1.4871e-04	7.4267e-04	1.3433e-03	1.3849e-03
τ_1	3.2338e-03	2.3201e-03	2.4030e-03	2.3857e-03
τ_2	3.4017e-03	2.3523e-03	2.1828e-03	1.9808e-03
μ_1	4.0127e-03	4.0472e-03	6.3975e-03	1.3496e-02
μ_2	3.4688e-03	4.2423e-03	6.4681e-03	1.3530e-02

As a preliminary conclusion, these results provide quantitative data to estimate errors brought by the contact repeatability. In the effort to improve the contact repeatability, national metrology laboratories (NMIs) are well recognized to guaranty traceability of *S*-Parameters measurements [5]. On-going works are clearly oriented towards improving the probe to contact repeatability in the millimetre-wave (30 – 300 GHz) up to the THz regime [11]-[12]. As mentioned in the introduction, we focus on the microwave regime (up to 67 GHz) with ultimate objective to address accurate measurements on extreme impedance devices. In this effort, in the following, we study the impact of measurement uncertainties obtained in Tables 1 and 2 on the determination of complex impedances.

IV.   ERROR PROPAGATION ON COMPLEX IMPEDANCES

In this section, we propose to highlight limitations of conventional on-wafer probing stations to address accurate measurement of extreme impedances such as sub-fF (10^{-15} F) capacitance values. In particular, we extend the reflection coefficient (S_{11}) uncertainty error model developed by D. Rytting [10] to uncertainty impedance (Z) error model. From [10], the reflection coefficient magnitude uncertainty $\Delta|S_{11}|$ and phase-shift uncertainty $\Delta\Phi$ can be written as

$$\Delta|S_{11}| \approx \delta_1 + \tau_1|S_{11}| + \mu_1|S_{11}|^2 \qquad (2)$$

$$\Delta\phi \approx \arcsin\left(\frac{\Delta|S_{11}|}{|S_{11}|}\right) \qquad (3)$$

Fig. 3 shows the reflection coefficient magnitude uncertainty as a function of the S_{11} amplitude at 10 GHz for both Z-analysis and XYZ-analysis.
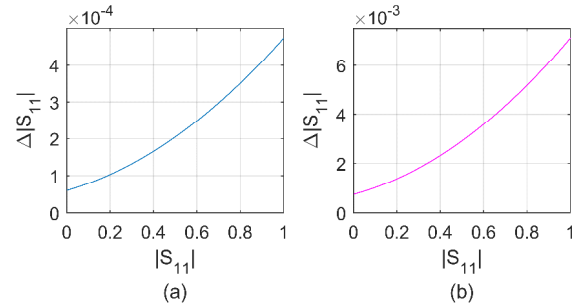

Fig. 3. Reflection coefficient magnitude uncertainty (a) Z-analysis (b) XYZ-analysis.

According to (2), the amplitude uncertainty increases as a function of S_{11} amplitude, as observed in Fig. 3. In particular, this implies that measurement of capacitances ($|S_{11}| = 1$) results in relatively large errors. For example, the phase-shift uncertainties computed from (3) at 10 GHz for ($|S_{11}| = 1$) are 0.027° and 0.4° for Z-analysis and XYZ-analysis

respectively. The Z-analysis generates significantly less measurement uncertainties than the XYZ-analysis.

In the following, we extend the work to uncertainty impedance (Z) error modelling. In [10], D. Rytting considers the worst-case uncertainty, where residual calibration error terms are collinear vectors added graphically (to provide maximum $\Delta|S_{11}|$ and $\Delta\phi$). Although this method provides the worst-case uncertainty in terms of complex reflection coefficient, we extend the method by considering a disk error with radius $\Delta|S_{11}|$ to propagate the full disk error on the Z-plane, with

$$Z = Z_0 \frac{1+S_{11}}{1-S_{11}} \quad \text{with} \quad Z_O = 50\,\Omega \qquad (4)$$

and therefore derive the measurement uncertainty in terms of complex impedance. Indeed, we investigate all combination values between reflection coefficient magnitude uncertainty and reflection coefficient phase uncertainty that provide maximum
Z-measurement uncertainty.

We consider the S_{11}-measurement uncertainty limited by a χ-disk defined by

$$\underline{\chi} = |\chi|e^{j\phi_\chi} \qquad (5)$$

with $\chi \in [0\,;\,\Delta|S_{11}|]$ and $\phi\chi \in [0\,;\,2\pi]$ (Fig. 4).
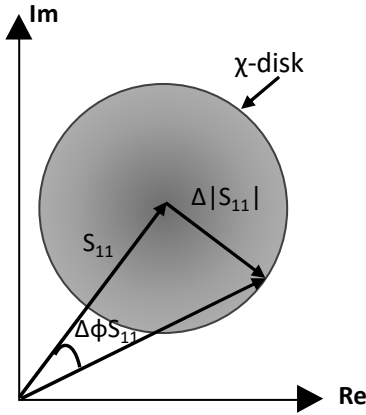
Fig. 4. Vector representation of the measurement uncertainty on the complex reflection coefficient S_{11}.

The χ-disk presented in Fig. 4 delimits the measurement error area on the complex reflection coefficient S_{11}. In the following, we consider a purely capacitive DUT and study the impact of the χ-disk on the determination of the capacitance value. First, we consider the determination of the measurement uncertainty on a capacitance of 320 fF $[Im(Z) = 50\Omega \text{ at } 10\,GHz]$ as follow:

- Compute the complex impedance $Z = \frac{1}{jCw}$ where $\omega = 2\pi f$ represents the angular frequency,
- Compute the complex reflexion coefficient $S_{11} = \frac{Z - Z_0}{Z + Z_0}$,
- Compute the reflection coefficient magnitude uncertainty $\Delta|S11|$ as given previously in (2),
- Compute the impedance uncertainty ΔZ using (6)

$$\Delta Z = Z_0 \left(\frac{1+S_{11}+\chi}{1-S_{11}-\chi} - \frac{1+S_{11}}{1-S_{11}} \right), \qquad (6)$$

- Compute the capacitance uncertainty ΔC using (7)

$$\Delta C = \frac{1}{j\omega(Z+\Delta Z)} - C. \qquad (7)$$

Fig. 5 shows the geometrical propagation of the χ-disk on the imaginary part $\Delta Im(Z)$ of the complex impedance Z considering both Z and XYZ analysis. The impact of the repeatability error between Z and XYZ analysis is highlighted with a degradation by one order of magnitude considering XYZ analysis. These results suggest that fine and repeatable probe to pads positioning are required to address accurate measurements of extreme impedances.
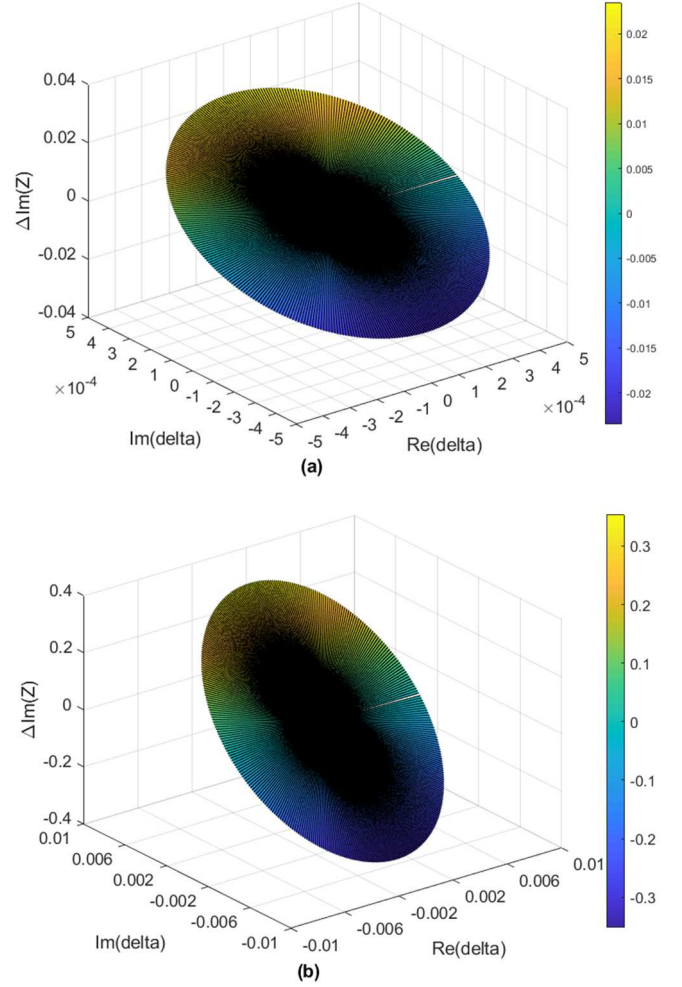
Fig. 5   Measurement uncertainty ΔIm(Z) computed by propagation of χ-disk on the complex impedance Z. (a) Z-analysis. (b) XYZ-analysis.

The impact on the determination of capacitance values is discussed in the following. First, we consider capacitance values down to 1 fF and compute the measurement uncertainties $\Delta Im(Z)$ and $\Delta Re(Z)$ at the test frequency 10 GHz (Table III).

TABLE III - MEASUREMENT UNCERTAINTY ON CAPACITANCES AT 10 GHz - Z-ANALYSIS AND XYZ-ANALYSIS

C(fF)	Δ|S11|		ΔIm(Z) (Ω)		ΔRe(Z) (Ω)	
	Z analysis ×10⁻⁴	XYZ analysis ×10⁻⁴	Z analysis	XYZ analysis	Z analysis	XYZ analysis
320	4.74	71	0.023	0.35	0.023	0.35
100	4.74	71	0.13	1.99	0.13	1.99
10	4.74	71	12	1.83×10^2	12	1.83×10^2
1	4.74	71	1204	6.73×10^4	1204	6.73×10^4

According to table III, the Z-analysis method shows better performances. As an example, for a capacitance value set to 320 fF, the relative measurement error introduced by the Z-analysis is 0.047% whereas the XYZ-analysis reaches 0.7%. It is also shown that for a capacitance (perfect imaginary impedance value), we introduce a measurement uncertainty on the real part $\Delta Re(Z)$ of the impedance. Consequently, $\Delta Re(Z)$ represents a series resistor with the capacitor. The RF measured impedance becomes $Z = 0.023\Omega + j(50 \pm 0.023)$ at 10 GHz.

Table IV provides the capacitance measurement uncertainties for the different cases considered.

TABLE IV - MEASUREMENT CAPACITANCES UNCERTAINTIES AT 10 GHz - Z-ANALYSIS AND XYZ-ANALYSIS

C(fF)	ΔC (F)		ΔC/C (%)	
	Z analysis	XYZ analysis	Z analysis	XYZ analysis
320	1.51×10^{-16}	2.26×10^{-15}	0.047	0.7
100	8.26×10^{-17}	1.23×10^{-15}	0.082	1
10	7.47×10^{-17}	1.03×10^{-15}	0.75	10
1	7.03×10^{-17}	8.09×10^{-16}	7.03	81

From table IV, it is clearly shown that conventional on-wafer probe stations are not suitable to measure accurately high impedance devices such as sub-fF capacitors. For example, a capacitance value of 1 fF measured at 10 GHz is measured with an error around 80 %. The Z-analysis demonstrates that, if the X and Y movements of the probe are theoretically controlled, the error can be reduced to ~7%. In addition, the Z-movement should be improved to foresee measurement of sub-fF capacitances values. In our previous works, we have tackled the issue of high impedance measurements by considering a two-port measurement configuration that is less insensitive to positioning errors [2]. Although accurate measurements on sub-fF55-nm MOS RF voltage-tunable capacitors have been addressed, the technique only suitable for one-port devices (configured in two-port measurements) cannot be used for high impedance two-port networks characterization. In Section V, we introduce our preliminary work regarding a new generation of nanorobotics on-wafer probing station that is based on the progress in the field of scanning probe microscopy (SPM) that employ piezo-positioning stages for decades [13]-[16].

V. AUTOMATED ON-WAFER PROBING STATION

The results presented in this paper have shown that mechanical displacements of the probe and particularly the repeatability of the GSG probe to device pads impact drastically the measurement uncertainty, in particular when impedances far from the VNA impedance 50 Ω are considered. We have proven that conventional on-wafer probing systems have a limited repeatability and cannot ensure reliable results with extreme impedance DUTs. To tackle this urgent issue, we are currently developing an automated probe station based on piezo-electrical nano-positionning stages. The GSG probes and chuck are both mounted on closed-loop piezo-base nano-positioners to reach nm positioning accuracy. These positioners are fully automated and controlled under LabVIEW® software. Real time image processing of probe landing into the DUT is under development to perform accurate, precise and repeatable alignment and tilt correction of the GSG probes, under MATLAB® software. Uncertainty measurements and calibrations will be done with VNA Tools II®. Fig. 5 gives an overview of the nanorobotics on-wafer probing system. Table shows the mechanical specifications of the system.
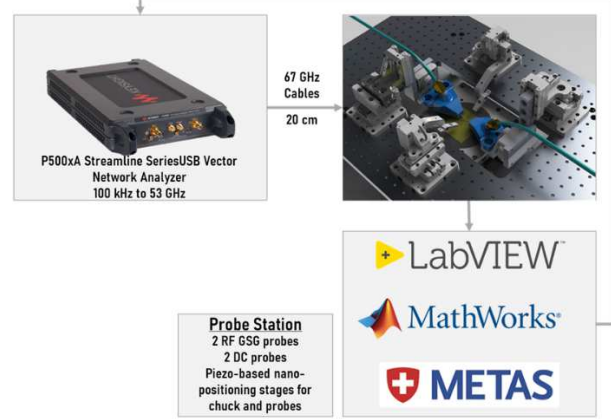

Fig. 6 Nanorobotics on-wafer probing system developed at IEMN.

TABLE V - GENERAL SPECIFICATIONS OF THE IEMN NANOROBOTICS ON-WAFER PROBING STATION.

	Z	XY	θ
Travel	21 [mm]	16 [mm]	∞
Max Normal Force [N]	30	20	3
Max Lift Force [N]	>1.5	1,5	-
Dimensions L x W x H [mm]	30 x 17 x 8.5	30 x 24 x 10,5	23,5 x 20 x 10,2
Resolution	>1 [nm]	>1 [nm]	>4 [µ°]

VI. CONCLUSION

This work investigates the measurement performance of conventional on-wafer probing system based on mechanical displacements. Two measurements methods have been considered, (i) based on single axis probe displacement Z, (ii) based on three axis probe displacements XYZ. The conducted study reports demonstrated the measurement performance degradation between the two analysis. In particular, we have proven that controlling the probe alignment in the XY axis improves the measurement repeatability and hence, reduces the impedance measurement uncertainty in the microwave range up de 20 GHz. This repeatability study comes as a preliminary work to justify the development of a new nanorobotics on-wafer probing

system. In future works, performance comparison with conventional on-wafer probing system will be considered. The future works will benefit from VNA Tools II® software to derive the measurement uncertainties.

REFERENCES

[1] The International Technology Roadmap for Semiconductors, Executive summary, 2013.

[2] K. Daffé, G. Dambrine, C. Durand, C. Gaquière and K. Haddadi, "On-Wafer Series-Through Broadband Measurement of Sub-fF55-nm MOS RF Voltage-Tunable Capacitors," *in IEEE Microwave and Wireless Components Letters*, vol. 28, no. 9, pp. 831-833, Sept. 2018.

[3] D. F. Williams, J. Cheron, B. Jamroz and R. Chamberlin, "On-Wafer Transistor Characterization to 750 GHz – the Approach, Results, and Pitfalls," 2018 *IEEE BiCMOS and Compound Semiconductor Integrated Circuits and Technology Symposium (BCICTS)*, 2018, pp. 1-5.

[4] A. Rumiantsev and R. Doerner, "RF Probe Technology: History and Selected Topics," *in IEEE Microwave Magazine*, vol. 14, no. 7, pp. 46-58, Nov.-Dec. 2013.

[5] U. Arz, et al., Best Practice Guide for Planar S-Parameter Measurements using Vector Network Analysers, Berlin, Germany:EURAMET, September 2018.

[6] R. G. Clarke, J. Quraishi and N. M. Ridler, "A bilateral comparison of on-wafer S-parameter measurements at millimeter wavelengths", *69th ARFTG Conf. Dig.* , Apr. 2007.

[7] R. Sakamaki and M. Horibe, "Realization of accurate on-wafer measurement using precision probing technique at millimeterwave frequency", *IEEE Trans. Inst. Meas.*, vol. 67, no. 8, pp. 1940-1945, 2018.

[8] K. Daffe et al., "On-Wafer Broadband Microwave Measurement of High Impedance Devices-CPW Test Structures with Integrated Metallic Nano-Resistances," 2018 *48th European Microwave Conference (EuMC)*, 2018, pp. 25-28.

[9] G. N. Phung et al., "Influence of Microwave Probes on Calibrated On-Wafer Measurements," *in IEEE Transactions on Microwave Theory and Techniques*, vol. 67, no. 5, pp. 1892-1900, May 2019.

[10] D. K. Rytting, "Network Analyzer Accuracy Overview," *58th ARFTG Conference Digest*, 2001, pp. 1-13.

[11] F. Mubarak, C. D. Martino, R. Toskovic, G. Rietveld and M. Spirito, "Automated Contacting of On-Wafer Devices for RF Testing," *2020 Conference on Precision Electromagnetic Measurements (CPEM)*, 2020, pp. 1-2.

[12] R. Sakamaki and M. Horibe, "Precision Adjustment of Probe-Tilt Angle With RF Signal Detection Technique," *in IEEE Transactions on Instrumentation and Measurement, vol. 69, no. 10, pp. 8500-8505, Oct. 2020.*

[13] K. Haddadi, C. Brillard, G. Dambrine and D. Théron, "Sensitivity and accuracy analysis in scanning microwave microscopy," *2016 IEEE MTT-S International Microwave Symposium (IMS)*, 2016, pp. 1-4.

[14] J. Li, Z. Nernati, K. Haddadi, D. C. Wallace and P. J. Burke, "Scanning Microwave Microscopy of Vital Mitochondria in Respiration Buffer," *2018 IEEE/MTT-S International Microwave Symposium - IMS*, 2018, pp. 115-118.

[15] K. Haddadi et al., "Combined scanning microwave and electron microscopy: A novel toolbox for hybrid nanoscale material analysis," *2017 IEEE MTT-S International Microwave Workshop Series on Advanced Materials and Processes for RF and THz Applications (IMWS-AMP)*, 2017, pp. 1-3.

[16] G. Sassine et al., "Memristor device characterization by scanning microwave microscopy," *2017 International Conference on Manipulation, Automation and Robotics at Small Scales (MARSS)*, 2017, pp. 1-4.

[17] M. Wollensack, J. Hoffmann, D. Stalder, J. Ruefenacht and M. Zeier, "VNA tools II: Calibrations involving eigenvalue problems," *2017 89th ARFTG Microwave Measurement Conference (ARFTG)*, 2017.